ICON-2, a Tissue Factor–Targeted Antibody-Drug Conjugate for the Treatment of Solid Tumors

Thi-Sau Migone, Jacques Gaudreault and Jan-Willem Theunissen

Iconic Therapeutics, South San Francisco, CA 94080

BACKGROUND

- Tissue factor (TF) expression is generally restricted in normal tissues due to its role in the coagulation cascade; however, membranous TF is frequently highly expressed in solid tumors and has been associated with poor prognosis.[1] Surface TF has been shown in gastrointestinal, head & neck, cervical, ovarian, bladder, lung, breast and other types of solid tumors. Membrane TF undergoes rapid internalization once bound by an antibody, making it an attractive target for antibody drug conjugates (ADCs). However, previously reported anti-TF antibodies have interfered with clotting by affecting the binding of FVIIa to TF and/or the generation of the ternary complex between FVIIa/FX/TF. Recently, tisotumabvedotin, an anti-TF–targeting ADC, has shown promising results in both preclinical models and in the clinic, validating TF as a therapeutic target.[2–4] However, this molecule has the potential to interfere with the coagulation cascade and may have a narrow therapeutic window due to the toxicity profile of monomethyl auristatin E (MMAE)
- ICON-2 is an ADC that is designed to improve the therapeutic potential of ADCs that target TF

METHODS

- **Antibody discovery and selection:** Human antibodies against human TF were isolated from a full-length human immunoglobulin G (IgG) library using an in vitro yeast selection system. TF-binding monoclonal antibodies (mAbs) were enriched by incubating biotinylated TF-His monomers at different concentrations with antibody-expressing yeast cells followed by magnetic bead selection and fluorescence-activated cell sorting on a FACSAriaII cell sorter. Selected clones underwent light- and heavy-chain affinity maturation[5]
- **Cell-based binding**: For cell-based antibody binding, approximately 1.2 x 10^5 cells were incubated with a 12-point 1:3 dilution titration of anti–human TF IgG1 antibody starting at 250 or 100 nM for 2 h on ice. After 2 washes, cells labeled with anti-TF antibody were incubated for 30 min on ice with 150 nM of phycoerythrin (PE) F(ab')2 fragment goat anti–human IgG, Fc-gamma fragment–specific; and samples were analyzed on a flow cytometer
- **FXa conversion**: 5 x 10^4 MDA-MB-231 cells were plated in the presence of FX at a final concentration of 200 nM in a HEPES buffer with 1.5 mM $CaCl_2$, then incubated with a titration of the antibodies for 15 min at 37°C. Upon reconstitution of the binary TF:FVIIa complex with a final concentration of 20 nM of FVIIa, cells were incubated for 5 min at 37°C. After quenching the reaction with EDTA in a black 96-well plate, generated FXa was measured with 50 µM of SN-7 6-amino-1-naphthalenesulfonamide–based fluorogenic substrate (Haematologic Technologies, Essex Junction, VT, USA). Percent FXa generation in the presence of anti-TF antibody relative to a no-antibody control was reported
- **Thrombin generation assay**: The anti-TF antibodies were diluted and mixed with Normal Pooled Plasma (NPP). Relipidated TF was added to a 96-well assay plate, followed by addition of the antibody/NPP mixture. Directly after combining the relipidated TF with the antibody/NPP, thrombin generation was initiated by the addition of calcium and the thrombin substrate. STAGO software was used to report the following parameter: Peak IIa (highest thrombin concentration generated on the thrombin generation curve [nM])
- **Conjugation**: Antibody in PBS, pH 7.4 was reduced with 2–2.5 molar equivalents of Tris(2-carboxyethyl)phosphine. After 2 h at 37°C, the partially reduced antibody was cooled to room temperature and conjugated for 1 h to a molar excess of maleimidocaproyl-valine-citrulline-p-aminobenzoyloxycarbonyl-MMAE (MC-vc-PAB-MMAE) or ZymeLink Auristatin (ZLA) followed by quenching with N-acetyl-L-cysteine. The reaction was buffer exchanged into PBS to remove small molecular weight reagents
- **Cytotoxicity assay**: Anti-TF ADCs were serially diluted. A431 cells were incubated in the presence of anti-TF ADCs for 3 days, followed by lysis in CTG assay reagent. CTG luminescence was measured, and the mean and standard deviation of 4 replicates were graphed in Prism and calculated using a fourth-party logistics (4-PL) model
- **Cell line–derived xenograft (CDX) and patient-derived xenograft (PDX)**: The HPAF-II pancreatic carcinoma cell line and PDXs were implanted subcutaneously in the flank of athymic nude mice (Charles River Laboratories or Envigo). Animals were randomized and treated when the average tumor size was 200 mm^3. Body weight and tumor size assessments were performed biweekly. Animals were removed from study and euthanized once tumor size reached 1200 mm^3, skin ulceration was evident, or end of study was reached (day 30 or 42 depending on model)
- **Nonhuman primate (NHP) study**: Female cynomolgus monkeys (2–3 kg) were treated on Day 1 and 22 with varying doses of ADCs ranging from 1.5 to 18 mg/kg. Assessments: hematology, clinical chemistries, coagulation, pharmacokinetics (PK)/antidrug antibodies (ADA), ophthalmic examinations, histology, and histopathology. Necropsies were performed on Day 36

RESULTS

Figure 1. Cell-based binding assay. Cell-based binding was evaluated using the unconjugated anti-TF mAb titrated on the TF-expressing cell lines HCT-116 and A431. Graphs show mean of quadruplicate wells.

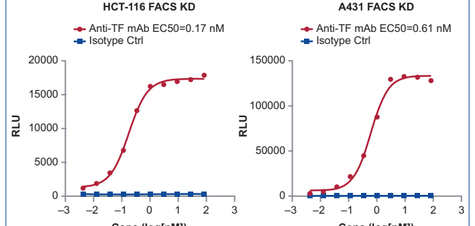

Conc, concentration; Ctrl, control; EC50, half-maximal effective concentration; FACS, fluorescence-activated cell sorting; KD, dissociation coefficient; mAb, monoclonal antibody; RLU, relative luminescence unit; TF, tissue factor.

Figure 2. Coagulation assays. Effects on coagulation cascade were assessed using a cell-based FXa conversion assay (left panel) and a thrombin generation assay (right panel). Thrombin generation was measured in NPP in the presence of relipidated TF and titrated antibodies. Peak IIa (highest thrombin concentration generated on the thrombin generation curve [nM]) is reported relative to plasma in the absence of antibody. For both assays, an FVII-competitor antibody is used as positive control.

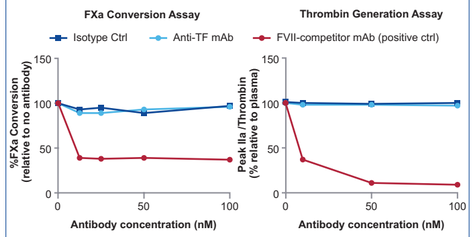

Ctrl, control; mAb, monoclonal antibody; NPP, normal pooled plasma; TF, tissue factor.

Figure 3. In vitro activity on A431 cell line. Graphs show mean and standard deviation of quadruplicate wells. The same anti-TF mAb was either conjugated to ZLA (to generate ICON-2) or to vc-MMAE as a comparator.

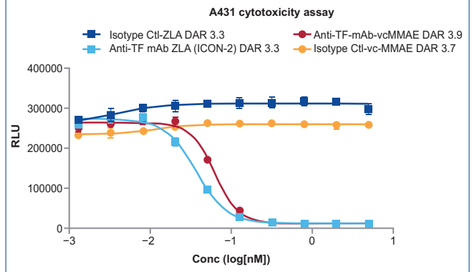

4-PL, fourth-party logistics; ADC, antibody-drug conjugate; mAb, monoclonal antibody; RLU, relative luminescence unit; TF, tissue factor; ZLA, ZymeLink Auristatin.

Figure 4. In vivo activity in HPAF-II xenograft model. The same anti-TF mAb was either conjugated to ZLA (to generate ICON-2) or to vc-MMAE as a comparator.

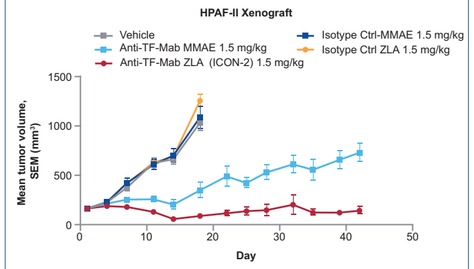

Ctrl, control; mAb, monoclonal antibody; MMAE, monomethyl auristatin E; SEM, standard error of the mean; ZLA, ZymeLink Auristatin.

Figure 5. Patient-derived xenografts. Immunohistochemistry of the PDX was performed using the anti-TF clone HTF-1 (ThermoFisher).

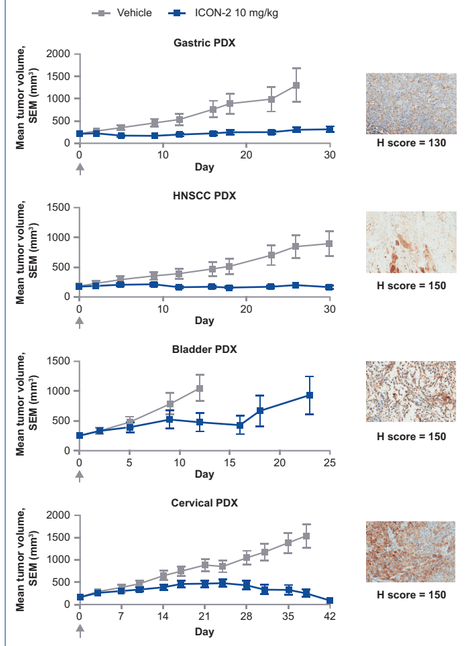

Ctrl, control; mAb, monoclonal antibody; MMAE, monomethyl auristatin E; PDX, patient-derived xenograft; SEM, standard error of the mean; TF, tissue factor; ZLA, ZymeLink Auristatin.

Table 1. Cynomolgus pilot study design and results.

ADC	Dose	Number of Animals	Dosing Days	Major Observations
Anti-TF-MMAE	1.5 mg/kg	3F	1, 22	N/A
Anti-TF-MMAE	3.0 mg/kg	3F	1, 22	Mild skin irritation and transient moderate decrease in neutrophils
Anti-TF-MMAE	6.0 mg/kg	3F	1, 22	Marked skin irritation requiring systemic steroids for 2 animals. Marked decrease in neutrophils
Anti-TF-ZLA	3.0 mg/kg	3F	1, 22	N/A
Anti-TF-ZLA	6.0 mg/kg	3F	1, 22	Mild skin irritation
Anti TF-ZLA	12.0 mg/kg	3F	1, 22	Mild skin irritation Transient mild AST elevation
Anti-TF-ZLA	18.0 mg/kg	3F	1, 22	Marked skin irritation requiring systemic steroids for 1 animal. Transient mild AST elevation

ADC, antibody-drug conjugate; AST, aspartate aminotransferase; F, female; MMAE, monomethyl auristatin E; TF, tissue factor; ZLA, ZymeLink Auristatin.

Figure 6. Neutropenia. Absolute neutrophil count was performed throughout the study on indicated days. Graphs show mean and SEM for 3 animals per timepoint. Grade 3 neutropenia (<500 cells/µL) was noted in 2/3 animals in the 6 mg/kg vc-MMAE group. No effect was observed in the ZLA groups. The historical average for the facility for female cynomolgus monkeys is 4.6 x 10^3/µL.

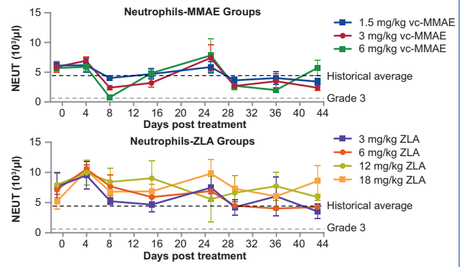

MMAE, monomethyl auristatin E; SEM, standard error of the mean; ZLA, ZymeLink Auristatin.

Table 2. Intact ADC PK parameters.

ADC	Dose Level	1st Dose C_{max}, µg/mL mean (SD)	1st Dose $AUC\text{-}0_{0\text{-}21}$, µg*d/mL mean (SD)	1st Dose $t_{1/2}$, days mean (SD)	2nd Dose C_{max}, µg/mL mean (SD)	2nd Dose $AUC\text{-}0_{0\text{-}42}$, µg*d/mL mean (SD)	2nd Dose $t_{1/2}$, days mean (SD)
Anti-TF-mAb-vcMMAE	1.5 mg/kg	31.6 (1.63)	38.4 (5.87)	1.12 (0.169)	15.8 (14.1)	16.4 (15.8)	0.820 (0.201)
Anti-TF-mAb-vcMMAE	3.0 mg/kg	57.1 (7.17)	88.9 (11.5)	1.34 (0.161)	39.2 (14.0)	26.4 (16.1)	0.582 (0.234)
Anti-TF-mAb-vcMMAE	6.0 mg/kg	157 (15.7)	265 (45.0)	1.64 (0.172)	99.2 (56.7)	103 (86.4)	0.957 (0.681)
Anti-TF-mAb-ZLA	3.0 mg/kg	68.1 (6.23)	214 (27.4)	1.91 (0.250)	59.4 (32.3)	170 (110)	1.39 (0.369)
Anti-TF-mAb-ZLA	6.0 mg/kg	165 (10.7)	511 (84.2)	2.23 (0.436)	152 (13.6)	302 (35.2)	2.26 (0.823)
Anti-TF-mAb-ZLA	12.0 mg/kg	281 (18.7)	1250 (86.7)	3.03 (0.589)	278 (22.4)	805 (118)	2.12 (0.179)
Anti-TF-mAb-ZLA	18.0 mg/kg	464 (24.5)	2000 (212)	5.10 (0.816)	378 (90.4)	2100 (205)	4.14 (0.410)

ADC, antibody-drug conjugate; AUC, area under the curve; C_{max}, peak concentration; MMAE, monomethyl auristatin E; PK, pharmacokinetics; SD, standard deviation; $t_{1/2}$, half-life.

CONCLUSIONS

- ICON-2 is an ADC that is designed to improve on the therapeutic potential of ADCs that target TF
- The anti-TF antibody in ICON-2 does not affect coagulation as measured by FXa conversion and thrombin generation assays, while still binding human and cynomolgus TF with high affinity
- ICON-2 is conjugated to the linker-payload ZLA (ZymeLink Auristatin), a novel auristatin payload that inhibits cell division by blocking the polymerization of tubulin but with potential for improved tolerability compared to vc-MMAE
- ICON-2 was more potent than the ADC generated with the same antibody conjugated to vc-MMAE in the HPAF-II tumor model
- In PDX models, ICON-2 showed excellent efficacy with significant tumor growth inhibition and, in some cases, complete regression
- Tolerability and exposure of ICON-2 was superior in a monkey study in which vc-MMAE and ZLA conjugated to the same antibody were compared
- These preclinical results support further development of ICON-2, and IND-enabling studies are currently ongoing

ABBREVIATIONS

4-PL, fourth-party logistics; ADC, antibody-drug conjugate; AUC, area under the curve; CDX, cell line–derived xenograft; C_{max}, peak concentration; Conc, concentration; Ctrl, control; EC50, half-maximal effective concentration; EDTA, ethylenediaminetetraacetic acid; FACS, fluorescence-activated cell sorting; HEPES, 4-(2-hydroxyethyl)-1-piperazineethanesulfonic acid; IgG, immunoglobulin G; KD, dissociation coefficient; IND, investigational new drug; mAb, monoclonal antibody; MC-vc-PAB-MMAE, maleimidocaproyl-valine-citrulline-p-aminobenzoyloxycarbonyl-monomethyl auristatin E; NHP, nonhuman primate; NPP, Normal Pooled Plasma; PBS, phosphate-buffered saline; PDX, patient-derived xenograft; PE, phycoerythrin; PK, pharmacokinetics; SEM, standard error of the mean; $t_{1/2}$, half-life; TF, tissue factor; ZLA, ZymeLink Auristatin

ACKNOWLEDGMENTS

The authors would like to acknowledge the support of Zymeworks, Iconic's technology partner; and Exelixis, the Company's financial partner for this program.

REFERENCES

1. van den Berg YW, et al. *Blood*. 2012;119:924–32.
2. Breij ECW, et al. *Cancer Res*. 2014;74:1214–26.
3. de Bono JS, et al. *Lancet Oncol*. 2019;20:383–93.
4. Hong DS, et al. *Clin Cancer Res*. 2020:1220–28.
5. Theunissen J-W, et al. *Mol Cancer Ther*. 2018;17:2412–26.

Corresponding author: Thi-Sau Migone, Head, Research, Iconic Therapeutics (Email: tmigone@iconictherapeutics.com)

Presented at World ADC Digital, September 15–18, 2020